J Solid State Electrochem (2012) 16:3079–3085
DOI 10.1007/s10008-012-1752-1

ORIGINAL PAPER

Synthesis and electrochemical performance of three-dimensionally ordered macroporous $LiCoO_2$

Juanjuan Peng · Tianjing Zhang · Hongmei Zhang · Zhiyong Zhang · Zhaohui Li · Gangtie Lei

Received: 1 January 2012 / Revised: 8 April 2012 / Accepted: 11 April 2012 / Published online: 26 April 2012

Abstract Three-dimensionally ordered macroporous (3DOM) $LiCoO_2$ was synthesized by colloidal crystal templating method using poly(methyl methacrylate) with the diameter of 232 nm as the template. The effects of roasting temperature on properties of $LiCoO_2$ cathode materials were investigated by thermogravimetric analysis (TG-DTG), scanning electron microscope, X-ray diffraction, transmission electron microscopy, and electrochemical measurements. The results indicated that the synthesized 3DOM $LiCoO_2$ calcined at 700 °C had better crystal framework and electrochemical properties. The 3DOM $LiCoO_2$ samples presented higher rate capacity compared to commercial $LiCoO_2$ with a specific discharge capacity of 151.2 mAh g^{-1} at a current density of 1 C, and 92 % of the specific discharge capacity was retained after 50 charge–discharge cycling.

Keywords Lithium-ion battery · Template · Three-dimensionally ordered macroporous (3DOM) · $LiCoO_2$

Introduction

$LiCoO_2$ is the prime lithium metal oxide used as cathode material for lithium-ion batteries, which still remains the foundation cathode material in many commercial lithium-ion cells because of its ease of production, excellent cycle stability, high volumetric energy density, good power rates, high specific capacity, and high operating cell voltage [1–3]. However, the traditional commercial $LiCoO_2$ battery suffers serious capacity loss when they are charged/discharged at a high rate. Polarization caused by slow diffusion of lithium ions and electrons in active materials is one challenging problem. To solve this problem, preparation of porous materials with highly ordered porous structures has been tried [4–6].

The three-dimensionally ordered macroporous structure can provide short diffusion pathways for Li^+ ions, which cause a faster Li^+ diffusion, improve the electrode/electrolyte contact, facilitate the deintercalation/intercalation of Li^+, enhance the utilization efficiency of the material, and reduce the polarization [7]. What is more is that the high porosity also reduces the effective current density at coordination current and ensures the structure stability during cycling [8]. The electrode materials with three-dimensionally ordered macroporous (3DOM) structure may be suitable for high-power lithium batteries, in which rapid charge and discharge are required. So far, 3DOM $LiCoO_2$ [9], V_2O_5 [10], $Li_4Ti_5O_{12}$ [11], Ni–Sn alloys [12], $LiFePO_4$ [13], and SnO_2 [14] have been applied in lithium-ion batteries.

Methods for shaping and structuring solids into functional objects have been developed and improved to create increasingly more complex features since the fabrication of early tools. The large and inhomogeneous grain sizes (>10 μm) of these electrode materials produced from solid-state techniques [15] would degrade the electrochemical performance of the electrode. The sol–gel method [16], Pechini process [17], polymer pyrolysis method [18], and fast microwave synthesis [19] could synthesize the samples in nanosize grain at low temperature, but these methods require long time and expensive initial reagents or involve complex preparative procedures. The colloidal crystal templating method is straightforward and quite general, and the prepared 3DOM material has less diffusional resistance to the active site, which is an attractive feature for cathode material for lithium-ion batteries.

J. Peng · T. Zhang · H. Zhang · Z. Zhang · Z. Li · G. Lei (✉)
Key Laboratory of Environmental-Friendly Chemistry and Application of Ministry of Education, College of Chemistry, Xiangtan University,
Xiangtan, Hunan 411105, China
e-mail: lgt@xtu.edu.cn

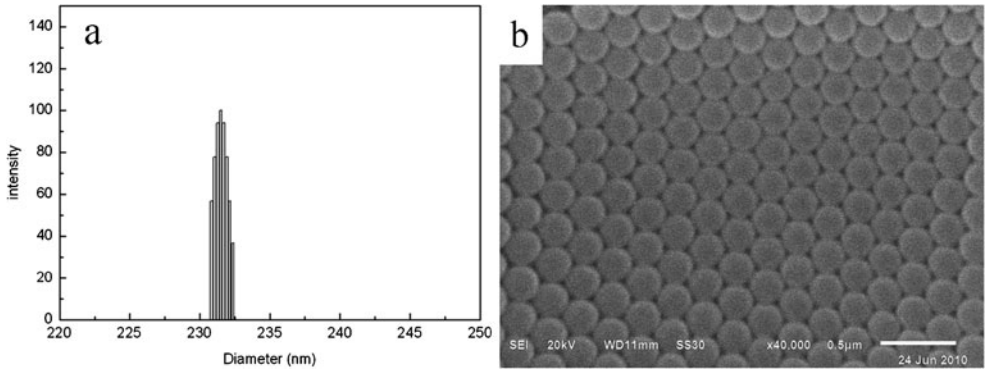

Fig. 1 DLS images (**a**) and SEM images (**b**) of PMMA crystal template

In this paper, 3DOM $LiCoO_2$ materials are prepared by colloidal crystal templating method using poly(methyl methacrylate) (PMMA) as the template. The effects of calcining temperature on properties of 3DOM $LiCoO_2$ cathode materials are investigated by scanning electron microscope (SEM), transmission electron microscopy (TEM), X-ray diffraction (XRD), galvanostatic charge–discharge, cyclic voltammogram (CV), and electrochemical impedance spectroscopy (EIS), respectively. The results show that the 3DOM $LiCoO_2$ calcined at 700 °C has a high discharge capability as well as cycling performance at high rate.

Experimental

Preparation of PMMA colloidal crystal template

The PMMA colloidal crystal templates are prepared by emulsion polymerization of methyl methacrylate monomer (MMA). First dissolved in 250 mL deionized water is 0.01 g sodium dodecyl sulfate used as the surfactant, then 35 g monomer (MMA) and 0.28 g potassium peroxodisulfate as the initiator are added to the above solution under continuous stirring. The mixed solution is bubbled by nitrogen for 20 min to remove oxygen in the reflux system. Then, the mixture is stirred and refluxed at 70 °C for 2.5 h. The colloidal crystal template is obtained by centrifugation and evaporating water.

Preparation of three-dimensionally ordered macroporous $LiCoO_2$

$Co(NO_3)_2{\cdot}6H_2O$ and $LiNO_3$ are used as the starting materials and dissolved in 50 mL ethanol in a molar ratio of 1:1, then 10 g dry PMMA colloidal crystal template is soaked for 10 min in the ethanol solution. And excess of this precursor solution is filtered off by vacuum filtration, and then the powder is dried at 50 °C for 12 h to form the precursor. Finally, the precursor is sintered at various temperatures in air.

Physical characterization

The size distribution of PMMA colloidal crystal template is determined by dynamic light scattering (DLS; Brookhaven BI-200SM). The morphologies and particle sizes of the samples are observed by transmission electron microscopy (TEM, JEOL JEM 2100) and scanning electron microscope (SEM, JEOL JSM 6610). Thermogravimetric–differential

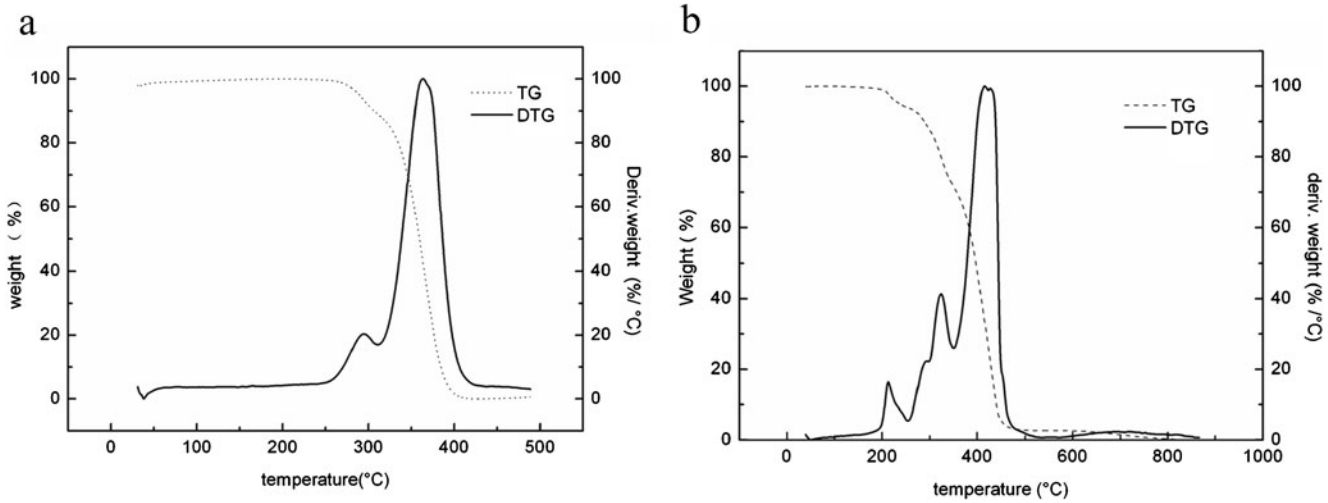

Fig. 2 TG-DTG curves of PMMA template (**a**) and 3DOM $LiCoO_2$ precursor (**b**)

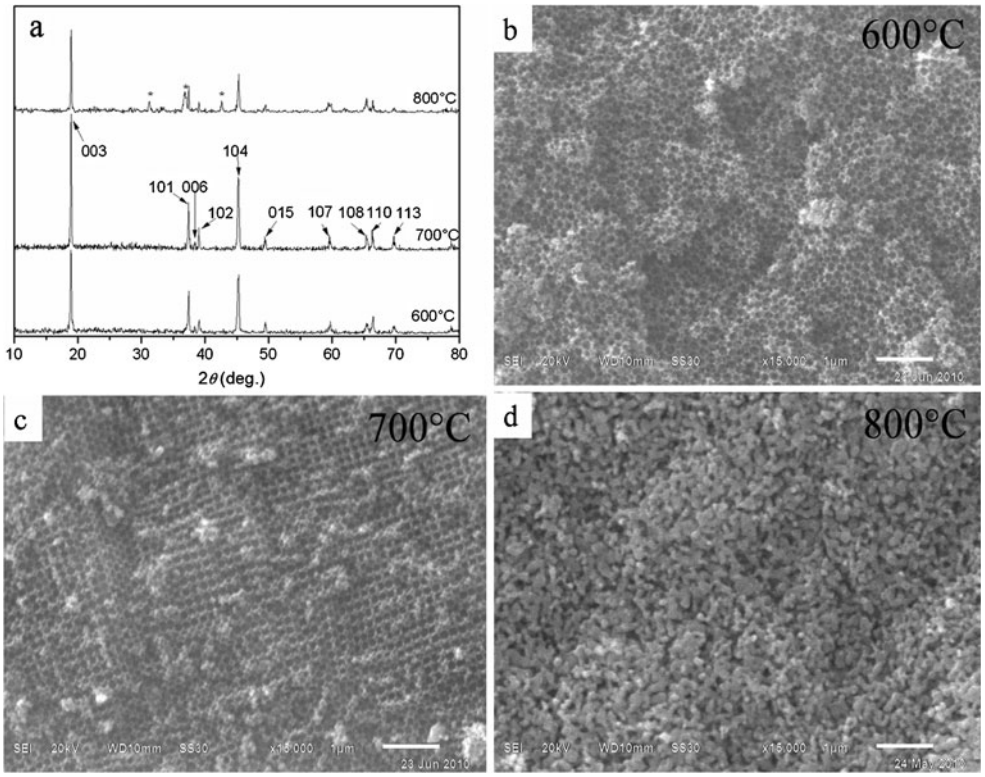

Fig. 3 Powder X-ray diffraction patterns (**a**) and SEM images (**b**–**d**) of synthesized 3DOM $LiCoO_2$ at various temperatures

thermogravimetric (TG-DTG) analysis of the precursor is investigated on an America TA company SDTQ 600 thermoanalyzer at the temperature range from 25 to 900 °C in air with a heating rate of 10 °C min^{-1}. The samples are characterized by X-ray powder diffraction analysis (XRD) using Cu Kα_1 radiation (40 kV and 40 mA) at a scan rate of 2° min^{-1} in the 2θ range from 10° to 90° (Rigaku D/MAX-2550). The porous properties were determined by nitrogen adsorption at 77 K using an NOVA-2100e instrument from Quantachrome. The test sample was evacuated at 120 °C under 0.1 Pa prior adsorption.

Electrochemical measurements

The electrodes are made by dispersing 80 wt% active materials, 10 wt% polyvinylidene fluoride binder and 10 wt% carbon black in *N*-methylpyrrolidone solvent to form a homogeneous slurry. The slurry is then coated uniformly on an Al foil. After vacuum drying at 120 °C for 12 h, the electrode disks are punched and weighed. The cells are assembled in an argon-filled glove box, using lithium metal foil as the counter electrode and reference electrode and Celgard 2400 as a separator. The electrolyte is 1 M $LiPF_6$ in a mixture of ethylene carbonate and dimethyl carbonate (1:1 by volume). The cells are charged and discharged over a voltage range of 3.0–4.3 V using a battery test system (BT-2000, Arbin Instruments Inc.). CV measurements of the cells are carried out using CHI660A (Chenghua, Shanghai). The sweep rate of CV is 0.1 mV s^{-1} over a voltage range of 3.0–4.5 V. EIS is conducted on EG&G 273 potentiostat/galvanostat system by applying an alter current amplitude of 5 mV in the frequency range of 100 kHz to 0.01 Hz at an open circuit voltage of 3.8 V (vs. Li/Li^+). The EIS data are fitted by Zview 2 software. All the potentials here after in the article are referred to lithium metal.

Table 1 Nitrogen sorption results: BET surface area, pore volume, and pore diameter

Temperature (°C)	S_{BET} (m^2 g^{-1})	Pore volume (cc g^{-1})	Pore diameter (nm)
600	24.17	0.032	24
700	27.5	0.065	25
800	22.41	0.047	23

Results and discussion

The solution of colloidal crystals is diluted with water and determined by DLS under the wavelength of 532 nm at room temperature. The results of DLS measurement in Fig. 1a indicate that PMMA latex spheres have narrow size distributions, with a diameter of ca. 232 nm. SEM images of PMMA colloidal crystal template synthesized by emulsion polymerization in Fig. 1b demonstrate that the template is a well-defined ordered closed packed arrays in three dimensions

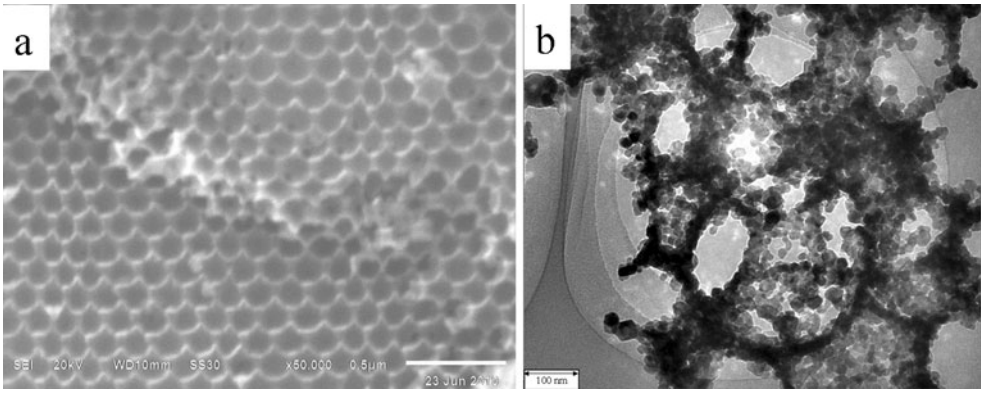

Fig. 4 SEM image (**a**) and TEM image (**b**) of 3DOM $LiCoO_2$ prepared at 700 °C

and the PMMA spheres are almost uniform, also showing that the diameters of the spheres are narrowly distributed.

TG-DTG is used to establish the temperature conditions. Figure 2a shows the weight loss of the PMMA colloidal crystal template. The template begins to decompose at 300 °C, corresponding to the peak in DTG curve. And the weight of PMMA is almost unchanged when the temperature is higher than 400 °C, which can be recognized to the completed decomposition of PMMA. In addition, the oxidation decomposition of PMMA in the temperature region of 200–250 °C is very quick and accompanied by the formation of a large number of gases. In this way, the heating rate should be slowly when preparing, in order to avoid the rapid burning of PMMA to destroy ordered macroporous framework. TG-DTG curves to find suitable calcinations' temperature for the synthesis 3DOM $LiCoO_2$ are shown in Fig. 2b. The weight loss before 200 °C is attributed to the evaporation of ethanol and water and release of water in crystallization. The second weight loss in the temperature region of 200–250 °C is accompanied by decomposition of nitrate. The third thermal event from 250 to 450 °C can be predicted by the formation of cobalt lithium oxide solid solution and pyrolysis of PMMA. When the precursor is heated to 500 °C, the single-phase $LiCoO_2$ begins to be produced. The weight of the precursor is almost unchanged after 500 °C, which may indicate that the reaction has been completed. In order to optimize the temperature condition for the synthesis of 3DOM $LiCoO_2$, a series of compounds are prepared with the results of TG-DTG analysis by calcinations at 250 °C for 1 h, 400 °C for 2 h, and then above 600 °C for 4 h by step.

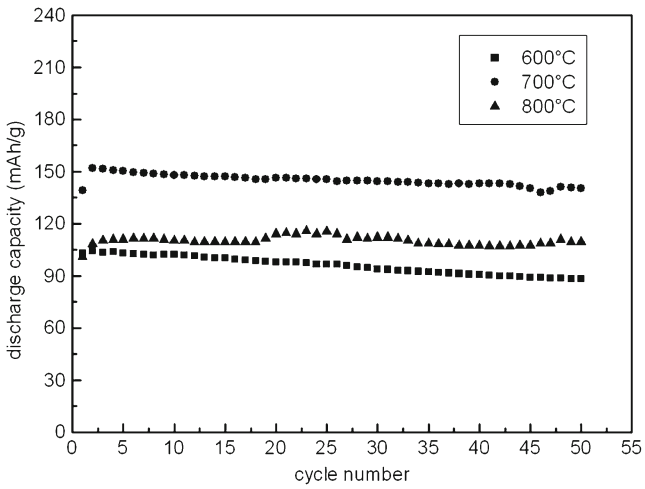

Fig. 5 The cycling performance of 3DOM $LiCoO_2$ samples at 1 C rate prepared at various temperature

Figure 3a represents the series of powder X-ray diffraction patterns of synthesized 3DOM $LiCoO_2$ with various temperatures. All materials have a rock salt structure with trigonal symmetry ($R\bar{3}m$). In the XRD pattern of $LiCoO_2$, the two split diffraction peaks (006) and (012) indicate the alternating lithium and cobalt layers structure [9]. When the integrated intensity ratio of the (003) to (104) peaks falls below 1.2, the (006) and (012) peaks are scarcely distinguishable from each other [20]. The ratios of (003) and (104) peaks in the samples prepared at 600, 700, and 800 °C are 1.391, 1.395 and 1.167, respectively. Therefore, being prepared at 600 and 700 °C, the samples have better crystal structure. With the temperature increasing to 800 °C, the two weakened diffraction peaks (006) and (012) suggest the incomplete alternating layers, what is more is that some Co_3O_4 impurity is formed in the sample (the corresponding reflections of Co_3O_4 impurity have been marked with triangles on the top pattern). Figure 3b–d shows the SEM images of 3DOM $LiCoO_2$ samples prepared at the indicated calcinations' temperatures. The sample prepared at 700 °C has better ordered mesopore structure than that at 600 °C due to the pore shrinkage associated with grains growth at higher temperatures. Pore interconnectivity and overall macroporosity are lost upon further heating to 800 °C. Furthermore, the specific surface area of the three materials calculated by the Brunauer–Emmett–Teller (BET) method and the pore volume determined by the Barrett–Joyner–Halenda approach are shown in Table 1, respectively. The results suggest the 3DOM $LiCoO_2$ material prepared at 700 °C has the highest specific surface. The sample

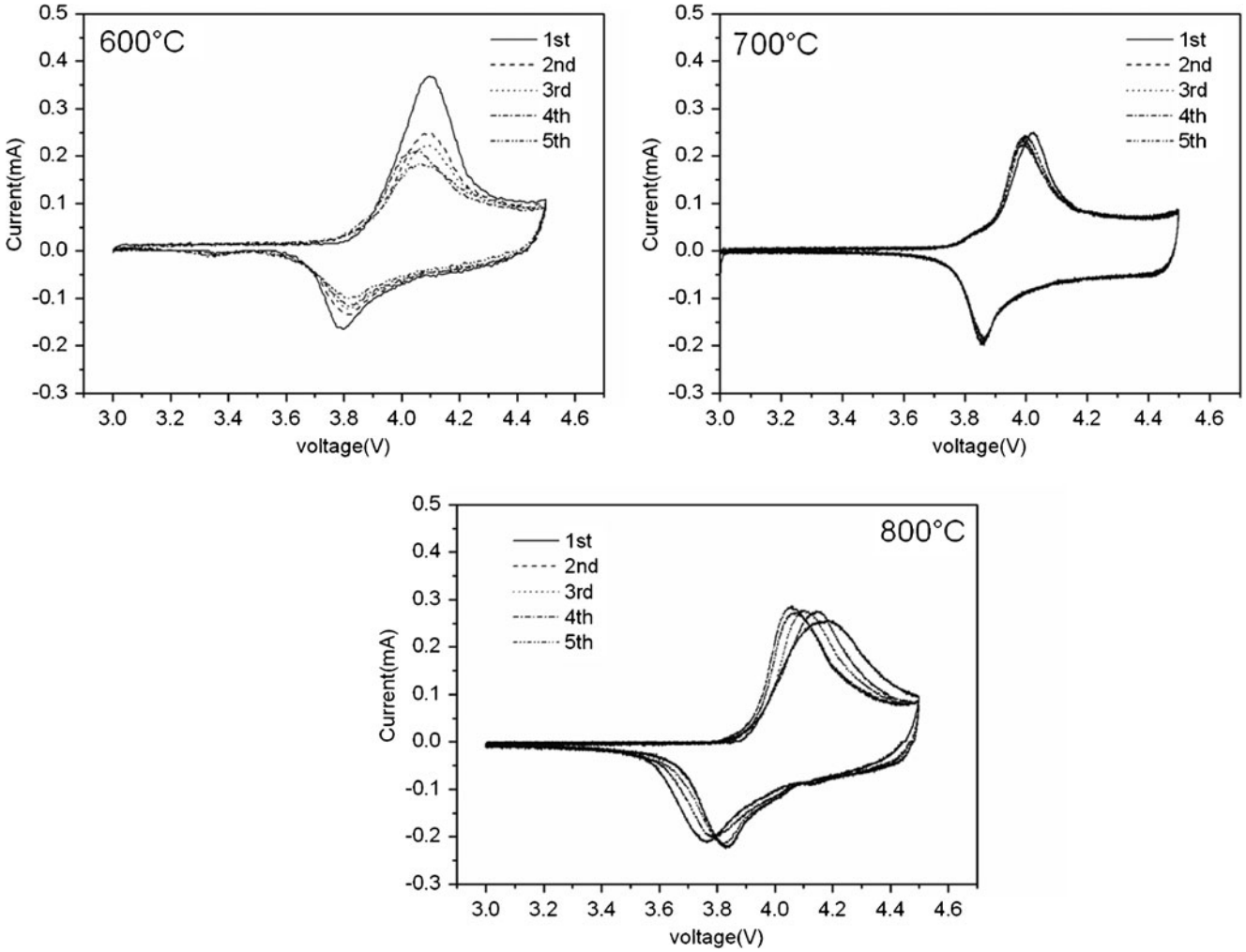

Fig. 6 The CV curves of 3DOM $LiCoO_2$ sample synthesized at various temperatures with a scan rate of 0.1 mV s^{-1}

synthesized at 700 °C maintains suitable macroporous structure and shows the best crystal structure because of the maximized intensity ratio of diffraction peaks (003) and (104).

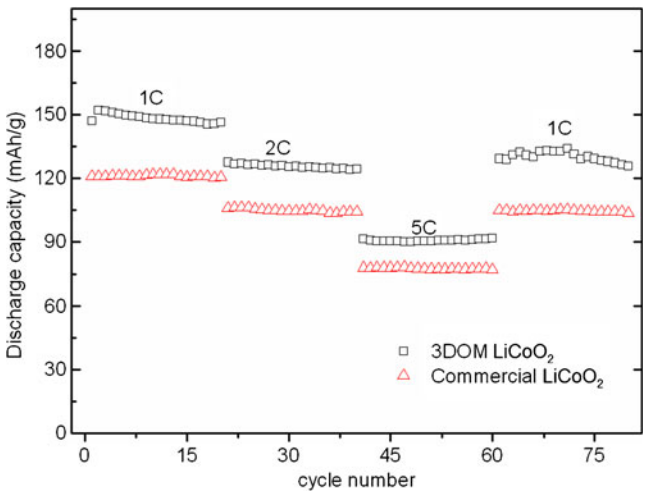

Fig. 7 The cycling performance of 3DOM $LiCoO_2$ prepared at 700 °C and commercial $LiCoO_2$ at different discharge rates between 3.0 and 4.3 V

High-resolution SEM and TEM micrographs of the prepared 3DOM $LiCoO_2$ at 700 °C are shown in Fig. 4. It shows that the sample has formed the typical inversed opal structure, and the PMMA template is replaced by macropores. The center-to-center average distance between the pores is 119±10 nm, and the thickness of the pore wall consisted of nanocrystal $LiCoO_2$ is between 20 and 30 nm. The round channels confirm that the mesopores in the prepared $LiCoO_2$ connected with each other.

Accordingly, the Li/$LiCoO_2$ cells are assembled and battery performance of 3DOM $LiCoO_2$ samples synthesized at various temperatures at 1 C rate over a voltage range of 3.0–4.3 V are shown in Fig. 5. The 3DOM $LiCoO_2$ prepared at 700 °C delivers the second specific discharge capacity of 151 mAh g^{-1}, which is largely higher than that of other materials exhibiting the second specific discharge capacity of 110 mAh g^{-1}. And the sample prepared at 700 °C possesses the best cycling stability for 92.7 % of the specific

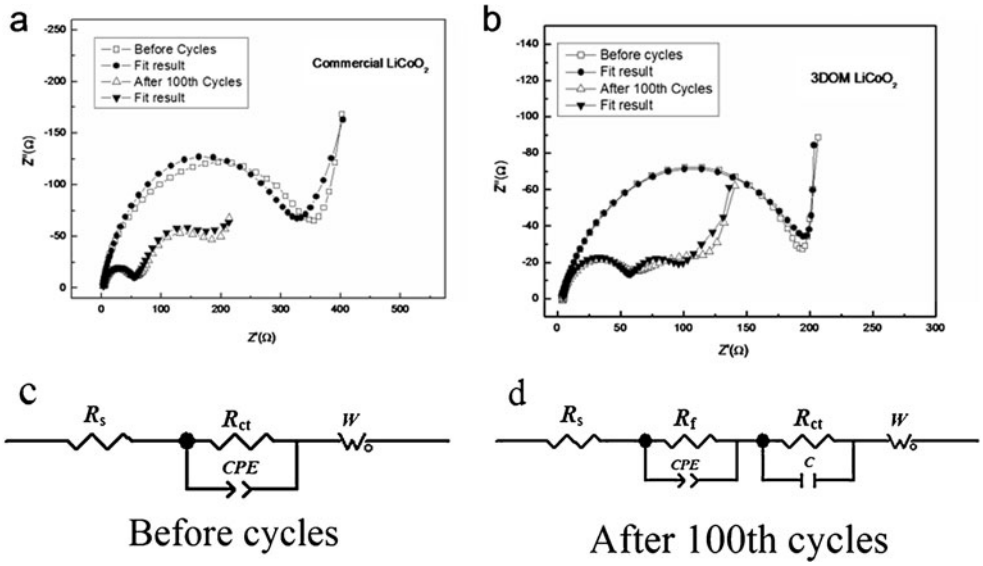

Fig. 8 **a**, **b** Nyquist plots of 3DOM $LiCoO_2$ prepared at 700 °C and commercial $LiCoO_2$ before cycles and after 100th cycles and **c**, **d** equivalent circuit diagram of EIS before cycles and after 100th cycles

discharge capacity retaining after 50 charge–discharge cycling. From the optimization, the temperature of 700 °C is found to be the better optimal condition to accomplish high-performance 3DOM $LiCoO_2$.

The cyclic voltammograms of 3DOM $LiCoO_2$ samples synthesized at various temperatures with a scan rate of 0.1 mV s^{-1} over a voltage range of 3.0–4.5 V are shown in Fig. 6. A single pair of the redox peaks is observed for all the samples. The CVs pictures all indicate an anodic peak around 4.1 V as well as the corresponding cathodic peak around 3.9 V, suggesting that the processes are reversible. Due to the crystal structure of materials prepared at 600 °C being not very integral compared with that at 700 °C, in the CV pattern, the integral area is gradually minished and the specific discharge capacity become low retention during cycling. At 800 °C, the diminished polarization of electrode led to the specific discharge capacity increase, which corresponding to the cycling performance plot. The sample prepared at 700 °C has smaller separation between the anodic and cathodic peaks, better superposition, and lesser polarization, which is representative of better kinetics and cycling stability.

Figure 7 represents the cycling performance of 3DOM $LiCoO_2$ prepared at 700 °C and commercial $LiCoO_2$ (Hunan Shanshan New Material Co., Ltd.) at different discharge rates between 3.0 and 4.3 V. The galvanostatic charge–discharge rate is increased gradually from 1 to 5 C and finally returned to 1 C. At any discharge rate, the specific discharge capacity of 3DOM $LiCoO_2$ is all along higher than that of commercial $LiCoO_2$. Especially after returning to a rate of 1 C for a second time, a specific discharge capacity of 125 mAh g^{-1} for 3DOM $LiCoO_2$ was obtained, which is higher than that of 90 mAh g^{-1} for commercial $LiCoO_2$ at 1 C. The result indicates the excellent cycling stability of the 3DOM $LiCoO_2$ cathode even after rather harsh loading/deloading rates.

The EIS measurements are performed for 3DOM $LiCoO_2$ prepared at 700 °C and commercial $LiCoO_2$ electrodes during before cycle and after 100th cycles. The impedance plots are shown in Fig. 8a, b, and the equivalent circuits before cycle and after 100th cycles used to fit the data are shown in Fig. 8c, d, respectively. In this equivalent circuit, R_s is the electrolyte resistance. R_f and CPE represent the resistance of solid electrolyte interface (SEI) film and constant phase elements. R_{ct} and C represent the charge transfer resistance and double layer capacitance. W is the Warburg impedance related to the diffusion of Li^+ ions. Both electrodes exhibit a semicircle in the high-frequency range and an inclined line in the low-frequency range. The high-frequency semicircle is assigned to the charge transfer impedance in the electrode/electrolyte interface, and the inclined line corresponds to the lithium-ion diffusion process [21–23]. Electrolyte, particle–particle, and charge transfer resistances of Fig. 8a, b are calculated using the equivalent circuit of Fig. 8c, d shown in Table 2. Before

Table 2 Electrolyte, particle–particle, and charge transfer resistances of Fig. 8a, b calculated using the equivalent circuit of Fig. 8c, d

Samples		R_s (Ω)	R_f (Ω)	R_{ct} (Ω)
Commercial LCO	Before cycle	1.767	–	347
	After 100th cycle	2.935	55.32	110.2
3DOM LCO prepared at 700 °C	Before cycle	3.009	–	207
	After 100th cycle	4.448	56.25	49.93

cycling, the charge transfer impedances for 3DOM $LiCoO_2$ and commercial $LiCoO_2$ electrodes are 347 and 207 Ω, respectively, which illustrates the charge transfer impedances decreasing greatly. After 100th cycles, the electrodes have two semicircles; the high-frequency semicircle is attributed to SEI film and contact resistance, and the semicircle in medium frequency is the charge transfer impedance [22]. The values of R_f are 55.32 and 56.25 Ω, respectively, which shows the similar SEI film and contact resistance. However the value of R_{ct} in medium frequency decreasing from 110.2 to 49.93 Ω suggests the sharply decreased charge transfer impedance in 3DOM $LiCoO_2$ material. The structure of three-dimensionally ordered macroporous in $LiCoO_2$ could shorten the diffusion pathway of lithium ions and decrease charge transfer impedances, and improve the cycling performance at a high rate.

Conclusion

3DOM $LiCoO_2$ is synthesized by colloidal crystal templating method using PMMA with the diameter of 232 nm as the template. XRD analysis indicates that the synthesized 3DOM $LiCoO_2$ calcined at 700 °C has better crystal framework and owns the typical inverse opal structure. As SEM and TEM images shown, the macropore diameters of the $LiCoO_2$ are about 150 nm and the pore wall thickness are between 20 and 30 nm. The 3DOM $LiCoO_2$ samples presented higher rate capacity with a second specific discharge capacity of 151.2 mAh g^{-1} at a current density of 1 C, and 92 % of the specific discharge capacity is retained after 50 charge–discharge cycling. Compared to commercial $LiCoO_2$, 3DOM $LiCoO_2$ shows the excellent cycling stability after rather harsh loading/deloading rates and the greatly decreased charge transfer impedances.

Acknowledgments This work was financially supported by the National Natural Science Foundation of China (21174119) and the Science and Technology Planning Project of Hunan Province, China (No. 2008FJ3097).

References

1. Patil A, Patil V, Shin D, Choi J, Paik D, Yoon S (2008) Mater Res Bull 43:1913–1942
2. Bates JB, Dudney NJ, Neudecker BJ, Hart FX, Jun HP, Hackney SA (2000) J Electrochem Soc 147:59–70
3. Scrosati B, Garche J (2010) J Power Sources 195:2419–2430
4. Jiao F, Shaju KM, Bruce PG (2005) Angew Chem Int Ed 44:6550–6553
5. Wu YP, Wan CR, Jiang CY, Fang SB (2002) Lithium ion secondary batteries. Chemical Industry Press, Beijing, pp 103–106
6. Liu H, Fu LJ, Zhang HP, Gao J, Li C, Wu YP, Wu HQ (2006) Electrochem Solid-State Lett 9:A529–A533
7. Aricò AS, Bruce PG, Scrosati B, Tarascon JM, Schalkwijk WV (2005) Nat Mater 4:366–377
8. Qu QT, Fu LJ, Zhan XY (2011) Energy Environ Sci 4:3985–3990
9. Ergang NS, Lytle JC, Yan H, Stein A (2005) J Electrochem Soc 152:A1989–A1995
10. Li ZH, Tang JJ, Yang J, Cheng C (2011) Funct Mater Lett 4:61–64
11. Shao D, He JR, Luo Y, Liu W, Yu XY (2011) Synthesis and electrochemical performance of nanoporous $Li_4Ti_5O_{12}$ anode material for lithium-ion batteries. J Solid State Electrochem. doi:10.1007/s10008-011-1604-4
12. Woo SW, Okada N, Kotobuki M (2010) Electrochim Acta 55:8030–8035
13. Doherty CM, Caruso RA, Smarsly BM, Drummond CJ (2009) Chem Mater 21:2895–2903
14. Yim CH, Baranova EA, Courtel FM, Abu-Lebdeh Y, Davidson IJ (2011) J Power Sources 196:9731–9736
15. Ermete A (2004) Solid State Ionics 170:159–171
16. Tang W, Liu LL, Tian S, Li L, Yue YB, Wu YP, Guan SY, Zhu K (2010) Electrochem Commun 12:1524–1526
17. Grigorova E, Mandzhukova T, Khristov M, Yoncheva M, Stoyanova R, Zhecheva E (2011) J Mater Sci 46:7106–7113
18. Xiao L, Yang Y, Zhao Y, Ai X, Yang H, Cao Y (2008) J Solid State Electrochem 12:149–153
19. Subramanian V, Chen CL, Chou HS, Fey GTK (2001) J Mater Chem 11:3348
20. Choi YM, Pyun SI, Moon SI, Hyung YE (1998) J Power Sources 72:83–90
21. Huang XH, Tu JP, Zhang CQ, Chen XT, Yuan YF, Wu HM (2007) Electrochim Acta 52:4177–4281
22. Takahashi M, Tobishima SI, Takei K, Sakurai Y (2002) Solid State Ionics 148:283–289
23. Yang SB, Song HH, Chen XH (2006) Electrochem Commun 8:137–142